Experimental Measurement of Impact Response in Carbon/Epoxy Plates

Yibo Qian* and Stephen R. Swanson†
University of Utah, Salt Lake City, Utah

The response of carbon/epoxy laminates to transverse impact is of considerable importance due to the susceptibility of these materials to delamination and fiber breakage under impact loading. Experiments and simple analytical approaches are desired for understanding the behavior during impact. In the present study, emphasis was placed on establishing scaling rules for relating laboratory-scale experiments to impacts on larger structures. The scaling rules were first derived from the governing differential equations of the linear impact response problem. Impact experiments were then carried out on AS4/3501-6 carbon/epoxy plates with the plate dimensions, projectile dimensions, and impact parameters all varied according to the scaling rules. The results were found to follow the scaling rules quite closely. A dynamic model of laminates subjected to impact was developed by using a Rayleigh-Ritz procedure. The predicted strain response agreed very well with the measured response, and supported the conclusions of the experiments regarding scaling rules.

I. Introduction

LAMINATED fiber composites are susceptible to impact damage due to their lack of through-the-thickness reinforcement. Since the impact resistance properties are not pure material properties, but instead are very much dependent on the dynamic structural behavior, an understanding of the dynamic response of composite structures subjected to impact loading is of great importance.

Impact tests on various composites have been conducted previously[1-5] providing evidence of reduction in strength and insight as to the modes of failure. A number of studies have been carried out on the impact response of laminated plates.[6-17]

The physical phenomena involved in the impact event include structural dynamic response, Hertzian contact effects (indentation), and both in-plane and through-the-thickness wave phenomena. The relative importance of these various effects depends upon the characteristics of both the impactor and the structure. It is, therefore, desirable to separate these effects.

Sun et al.[6-9] have performed a number of tests on laminated beams and plates, and have shown that the static indentation law is reasonably adequate in dynamic impact analysis. Daniel et al.[11] and Sun and Wang[7] have concluded that the in-plane membrane deformation is negligible, and that the deformation is dominated by bending. The influence of transverse shear deformation on behavior of laminated anisotropic structures can be expected to be large due to the lower transverse moduli. Whitney and Pagano[18] and Birman and Bert[19] confirmed that shear deformation is an essential factor influencing the behavior of laminated plates even in the fundamental mode.

Dobyns[14] has considered the analysis of thin simply supported orthotropic plates subjected to static and dynamic loading by assuming that the loading histories were known. In this case solutions for plate deflections, bending strains, and normal shear forces can be obtained easily by expanding the displacements, rotations, as well as the load in appropriate Fourier series. In general, however, the force history is not known but must be obtained as part of the solution. Boundary conditions other than simply supported have been analyzed by means of the Rayleigh-Ritz procedure, using assumed mode shapes based on combinations of the mode shapes for beams. The procedure has been outlined by Vinson and Sierakowski,[21] and recently employed by Cairns and Lagace.[15]

Because of the expense of testing large composite structures, it is very helpful to use structural scale model testing. However, the accuracy of this approach is open to question. Morton discussed the problems related to scaling of laminated fiber composites.[20] It was shown that generally complete scaling of a composite prototype is not possible. For example, the diameter of fibers and the thickness of individual laminae cannot be scaled. Also, in geometric scaling without explicit consideration of time effects, the change in time scale with geometric scaling may introduce differences in response due to viscoelastic effects in matrix deformation.

In order to evaluate the scaling rules, an experimental investigation was made into the impact response of carbon/epoxy plates. The plate dimensions, impactor dimensions, and impact parameters were all varied according to the scaling rules derived from the governing differential equations of the linear impact problem. An analytical model based on the Rayleigh-Ritz procedure was developed to predict the impact response of the specimens. The experimental and analytical results were compared with each other, and also compared with the scaling rules.

II. Scaling Rules

The scaling rules for a specially orthotropic laminated plate subjected to impact loading can be obtained from the following differential equations which govern the impact response[21]:

$$D_{11}\frac{\partial^2\bar{\alpha}}{\partial x^2}+D_{66}\frac{\partial^2\bar{\alpha}}{\partial y^2}+(D_{12}+D_{66})\frac{\partial^2\bar{\beta}}{\partial x\partial y}-A_{55}\left(\bar{\alpha}+\frac{\partial w}{\partial x}\right)=\frac{\rho h^3}{12}\frac{\partial^2\bar{\alpha}}{\partial t^2} \quad (1)$$

Received March 20, 1989; revision received June 26, 1989. Copyright © 1989 by the American Institute of Aeronautics and Astronautics, Inc. All rights reserved.

*Graduate Research Assistant, Department of Mechanical Engineering.
†Professor, Department of Mechanical Engineering.

$$(D_{12}+D_{66})\frac{\partial^2\bar{\alpha}}{\partial x\partial y}+D_{66}\frac{\partial^2\bar{\beta}}{\partial x^2}+D_{22}\frac{\partial^2\bar{\beta}}{\partial y^2}-A_{44}\left(\bar{\beta}+\frac{\partial w}{\partial y}\right)=\frac{\rho h^3}{12}\frac{\partial^2\bar{\beta}}{\partial t^2} \quad (2)$$

$$A_{55}\left(\frac{\partial\bar{\alpha}}{\partial x}+\frac{\partial^2 w}{\partial x^2}\right)+A_{44}\left(\frac{\partial\bar{\beta}}{\partial y}+\frac{\partial^2 w}{\partial y^2}\right)+p(t,x,y)=\rho h\frac{\partial^2 w}{\partial t^2} \quad (3)$$

This set of equations should describe the common features of a prototype and model if all of the variables are scaled from the prototype to the model. It is assumed that the layup can be scaled and that the variables may be related to each other by

$$T_p=\lambda_T T_m \quad (4)$$

in which T_p and T_m are typical variables such as displacements, strains, time, etc., for the prototype and the model, respectively, and λ_T is the scale factor related to these variables. For example, λ_x is length scale in the x direction. Substituting Eq. (4) into the first governing Eq. (1) yields

$$\left(\frac{\lambda_h^3\lambda_{\bar{\alpha}}}{\lambda_x^2}\right)D_{11}\frac{\partial^2\bar{\alpha}}{\partial x^2}+\left(\frac{\lambda_h^3\lambda_{\bar{\alpha}}}{\lambda_y^2}\right)D_{66}\frac{\partial^2\bar{\alpha}}{\partial y^2}+\left(\frac{\lambda_h^3\lambda_{\bar{\beta}}}{\lambda_x\lambda_y}\right)(D_{12}+D_{66})\frac{\partial^2\bar{\beta}}{\partial x\partial y}-(\lambda_h\lambda_{\bar{\alpha}})A_{55}\bar{\alpha}-\left(\frac{\lambda_h\lambda_w}{\lambda_x}\right)A_{55}\frac{\partial w}{\partial x}=\left(\frac{\lambda_\rho\lambda_h^3\lambda_{\bar{\alpha}}}{\lambda_t^2}\right)\frac{\rho h^3}{12}\frac{\partial^2\bar{\alpha}}{\partial t^2} \quad (5)$$

In the above, it has been assumed that the same material is being used, so that the in-plane stiffnesses A_{ij} scale as thickness and the bending stiffnesses D_{ij} scale as thickness cubed. Thus, the density will be unchanged, so that $\lambda_\rho=1$. The necessary condition of similitude between Eqs. (5) and (1) is the equality of the scaling factor products in parentheses in Eq. (5). This gives the following rules:

$$\frac{\lambda_x}{\lambda_y}=1,\quad \frac{\lambda_{\bar{\alpha}}}{\lambda_{\bar{\beta}}}=1,\quad \frac{\lambda_x}{\lambda_h}=1,\quad \frac{\lambda_w}{\lambda_h\lambda_{\bar{\alpha}}}=1,\quad \frac{\lambda_\rho\lambda_h^2}{\lambda_t^2}=1 \quad (6)$$

Following this procedure with Eqs. (2) and (3) gives three more rules:

$$\frac{\lambda_y}{\lambda_h}=1,\quad \frac{\lambda_w}{\lambda_h\lambda_{\bar{\beta}}}=1,\quad \frac{\lambda_\rho\lambda_x}{\lambda_w}=1 \quad (7)$$

By requiring strain similitude, we also have $\lambda_{\bar{\alpha}}=1$ and $\lambda_{\bar{\beta}}=1$. Combining Eqs. (6) and (7) results in the following scaling rules:

$$\frac{\lambda_x}{\lambda_h}=1,\quad \frac{\lambda_y}{\lambda_h}=1,\quad \frac{\lambda_w}{\lambda_h}=1,\quad \frac{\lambda_t}{\lambda_h}=1,\quad \lambda_\rho=1 \quad (8)$$

The above relations show that geometric scaling must be observed. Additionally, it should be noted that time must also be scaled. For example, if a plate prototype reaches full deflection after 100 ms, then a tenth scale model ($\lambda=0.1$) will reach its maximum deflection after 10 ms.

The total impact force on the plate can be obtained from the contact pressure $p(t,x,y)$:

$$F(t)=\iint_A p(t,x,y)\,dx dy \quad (9)$$

From the previous result, $\lambda_\rho=1$ in Eq. (8), it can be seen that if the contact area is geometrically scaled by λ^2, then the total force will also be scaled by λ^2. Similarly, the impact energy is found to be scaled by λ^3. If the impact velocity is the same for the prototype and the model, the mass of the impactor has to be scaled by λ^3.

In summary, if the geometry of plates is scaled as λ, the strain in the plates is constant with scaling if the impact velocity V_0 is unchanged. Also, the contact force scales as λ^2, and, if the contact area also scales geometrically, the contact pressure is unchanged. If the impactor also scales geometrically, the impactor mass scales as λ^3. Furthermore, the strain should increase linearly with impact velocity. A consideration of the time of response indicates that the time to maximum load and strain will scale as λ.

Even though the scaling rules derived above are for specially orthotropic laminated plates, the same scaling rules can be derived for plates with coupling terms. These scaling rules were also obtained by Morton[20] for laminated beams subjected to transverse impact loading, using dimensional analysis.

III. Experiments

A special compressed air gun has been developed for impact testing of composite plates. The schematic diagram for the setup is shown in Fig. 1. The projectiles used were cylinders with a hemispherical tip, instead of the more commonly used spherical projectiles. The use of cylindrical projectiles permitted the independent variation of projectile characteristics such as mass and impact tip diameter. It also facilitated a highly repeatable apparatus, as the impact velocity could be accurately controlled. This is believed to be due to the tighter seal which was obtained between the projectile and the barrel by using a cylindrical projectile as opposed to a spherical projectile. A light-emitting diode and photodetector were located near the end of the barrel to determine the velocity of the projectile. By adjusting the pressure of the compressed air in the tank of the air gun, the velocity of the projectile could be varied from 3–60 m/s (10–200 ft/s).

In order to evaluate the scaling rules derived previously, experiments were carried out to investigate the impact response of AS4/3501-6 carbon/epoxy plates which were furnished by Hercules Aerospace, Magna, Utah. The plates were geometri-

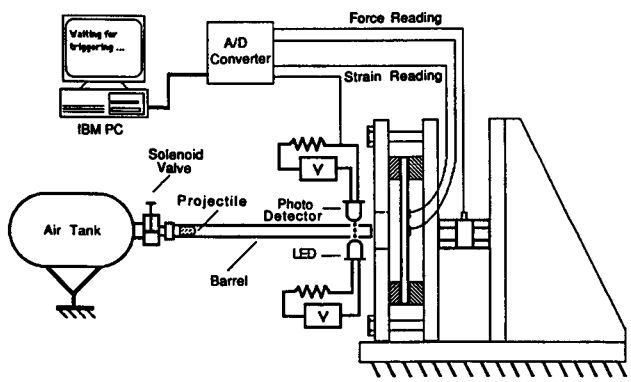

Fig. 1 Air gun impact test setup.

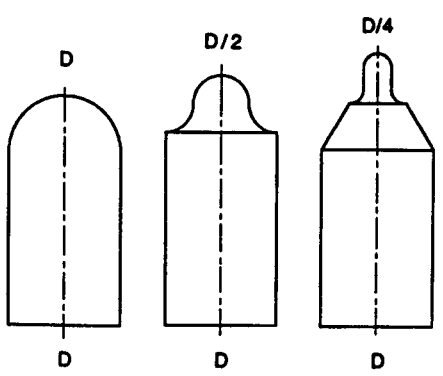

Fig. 2 Geometry of projectiles.

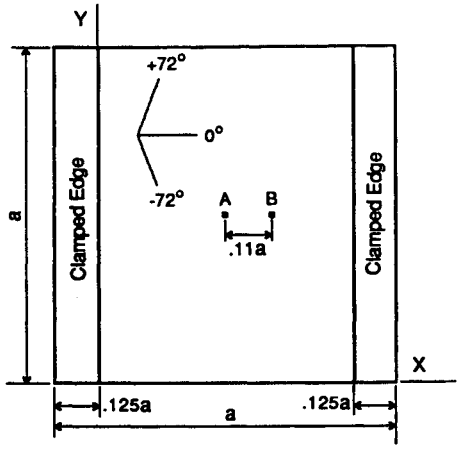

Fig. 3 Impact test specimen.

cally scaled in five sizes, from 50 mm × 50 mm × 1.072 mm thick (8 plies) to 250 mm × 250 mm × 5.36 mm thick (40 plies) (2 × 2 × 0.042 in. to 10 × 10 × 0.211 in.). If the scale factor is termed λ, the dimensions of the plates were thus scaled by λ = 1,2,3,4, and 5. The layup was $[(\pm 72)_\lambda/0_{2\lambda}]_s$. The projectiles used were constructed in five different diameters scaled as λ so that a total of five different barrel sizes were employed, with their inside diameters ranging from 6.4–31.8 mm (0.25–1.25 in.). The mass of each projectile varied from 2.86–358 gm (from 0.0063–0.79 lb), scaling as λ^3. For each projectile size, three tip diameters were used, their values being 1, ½, and ¼ of the corresponding barrel diameter. The geometry of the projectiles is shown in Fig. 2.

The plate specimens were clamped on two opposite edges and were free on the other two edges, as shown in Fig. 3. The clamping width was ⅛ of the plate size on each of two opposite edges. The clamped edges were normal to the 0-deg fibers, and the direction of these fibers was designated as the X-direction. The plates were instrumented with resistance strain gages, located behind the impact point (location A) and away from the impact center (location B) (Fig. 3). The size of the strain gages was scaled along with the plate sizes, in order to eliminate uncertainties with averaging the measured strain over the area of the gage. Impacts were performed with low velocities at 4.57 m/s (15 ft/s) to determine the structural response without damage, and also with velocities at 12.2, 18.3, and 24.4 m/s (40, 60, and 80 ft/s) to determine the extent of damage. Thus, 12 test conditions existed for each plate size, corresponding to the three different impactor tip diameters used at each of the four velocities. Four specimens were tested at each of these test conditions. All data were recorded with a high-speed digital data acquisition system.

IV. Dynamic Analysis

An understanding of the dynamic response of composite structures subjected to impact is necessary for design and also for the assessment of damage resistance. The scaling rules give the essential relationships between the dynamic responses of the prototype and model. A more detailed dynamic analysis is necessary to obtain a quantitative prediction of the plate response. The impact problem for plates has been considered by Tan and Sun,[9] Dobyns,[14] and Cairns and Lagace.[15] An exact solution is available for the simply supported case, if the contact indentation is neglected. As the present experiments used clamped-clamped and free-free boundary conditions on the opposite edges of the plate, a dynamic model has been developed using a Rayleigh-Ritz procedure to get an approximate solution.

In linear elastic plate theory,[22] the effect of transverse normal stress is assumed to be small and can be neglected. The effects of shearing deformation, in addition to bending-twisting coupling, and nonlinear contact behavior were included in the present model.

The analysis is based on Lagrange's equation of motion with the Lagrangian function $L = T - V$:

$$\frac{\mathrm{d}}{\mathrm{d}t}\frac{\partial L}{\partial \dot{x}} - \frac{\partial L}{\partial x} = 0 \tag{10}$$

where x is the modal amplitude.

Consider a laminated plate under dynamic lateral loading. The potential energy is given as

$$V = \frac{1}{2}\int\int_A [\kappa]^T[D][\kappa]\,\mathrm{d}A + \frac{1}{2}\int\int_A [\gamma]^T[A][\gamma]\,\mathrm{d}A - \int\int_A p(t,x,y)\,w(t,x,y)\,\mathrm{d}A \tag{11}$$

where the first two terms are bending and transverse shear strain energy, respectively, and the third is the work done by the lateral load. The notation follows that of Vinson and Sierakowski.[21] The kinetic energy of the plate is given by

$$T = \frac{\rho h}{2}\int\int_A \dot{w}(t,x,y)^2\,\mathrm{d}A \tag{12}$$

Here the in-plane and rotary inertia effects have been neglected, as suggested by Birman and Bert[19] and Dobyns.[14]

Because of the use of clamped boundary conditions on two opposing edges of the plate and free boundaries on the other two edges in the experiments, equations were developed using the Rayleigh-Ritz procedure. The procedure followed is based on choosing two series of functions, or "mode shapes," which satisfy the boundary conditions and give suitable expressions for deflection curves in x and y directions separately. The assumed deformed shape of the rectangular plate is then taken as a product of these functions. Therefore the series approximation for the planar rotations and transverse displacement can be taken as

$$\bar{\alpha}(t,x,y) = \sum_m\sum_n A_{mn}(t)X_m'(x)Y_n(y) \tag{13}$$

$$\bar{\beta}(t,x,y) = \sum_m\sum_n B_{mn}(t)X_m(x)Y_n'(y) \tag{14}$$

$$w(t,x,y) = \sum_m\sum_n C_{mn}(t)X_m(x)Y_n(y) \tag{15}$$

where A_{mn}, B_{mn}, and C_{mn} are the modal amplitudes of the plate and are to be determined. Substituting the assumed mode shapes in the expressions for potential and kinetic energy, and then using Lagrange's Eq. (10) gives three sets of equations with unknowns A_{mn}, B_{mn}, and C_{mn}. Substituting A_{mn}, B_{mn} in terms of C_{mn} yields a system of second-order

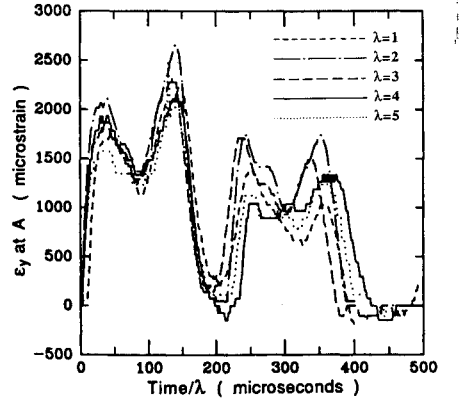

Fig. 4 Comparison of strain response at location A in impact tests on five different plate sizes, showing time scaling, V_0 = 4.57 m/s.

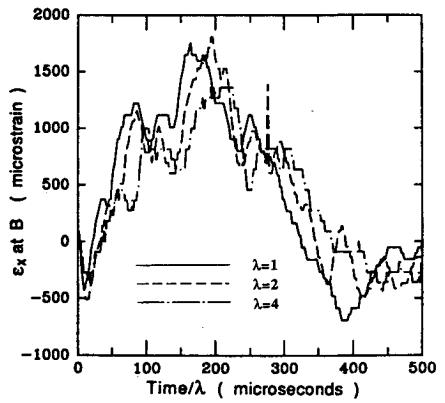

Fig. 5 Comparison of strain response at location B in impact tests on three different plate sizes, showing time scaling, $V_0 = 4.57$ m/s.

ordinary differential equations for the modal amplitudes C_{mn}

$$[S]\{\ddot{C}\} + [T]\{C\} = \{P\} \tag{16}$$

In the present study, the assumed mode shapes are taken as beam functions, which are solutions for mode shapes of beams under the appropriate boundary conditions.[23] The beam functions are orthogonal, permitting expansion of the load in terms of these functions. This expansion is of the form

$$p(t,x,y) = \sum_m \sum_n p_{mn}(t) X_m(x) Y_n(y) \tag{17}$$

with

$$p_{mn}(t) = \frac{\iint_A p(t,x,y) X_m(x) Y_n(y)\, dx dy}{\iint_A X_m^2(x) Y_n^2(y)\, dx dy} \tag{18}$$

The $\{P\}$ in the right-hand side of Eq. (16) is a force term, and each component comes from taking the derivative of the work done by the lateral load to the relative mode amplitude; that is,

$$P_{mn} = \frac{\partial W}{\partial C_{mn}} = p_{mn} \iint_A X_m^2(x) Y_n^2(y)\, dx dy \tag{19}$$

The contact force is assumed to be related to the contact indentation by the following equation, following Sun et al.[6-9]:

$$F = k\alpha^{3/2}$$

with

$$k = \frac{4}{3}\sqrt{R_s}\, E_{22} \tag{20}$$

where F is the total contact force on the plate, α is the local indentation, R_s is the radius of spherical impactor, and E_{22} is the transverse Young's modulus of the plate.

The contact force is then related to the motion of the projectile by assuming rigid-body dynamics for the projectile; that is

$$F = -m\ddot{u} \tag{21}$$

where m is the mass and u is the displacement of the projectile. The relationship between the local indentation, projectile displacement, and plate displacement at impact center is expressed by

$$\alpha(t) = u(t) - w(t,\xi,\eta) \tag{22}$$

where ξ and η give the location of the center of impact.

The contact pressure $p(t,x,y)$ is simply taken as the uniform distribution of the total contact force $F(t)$ over a square area A_c. This area is determined by

$$A_c = \pi[R_s^2 - (R_s - \alpha)^2] \tag{23}$$

The two sets of Eqs. (16) and (21) along with the contact laws given by Eqs. (20) and (22) were solved simultaneously. Because of the nonlinearity of the contact deformation relationship, the above equations were solved numerically, using the Newmark method with $\beta = 1/4$, which gives an unconditionally stable solution.

The constitutive properties utilized for the AS4/3501-6 carbon/epoxy lamina were

$E_{11} = 137.8$ GPa (20.0 Msi) $E_{22} = 11.02$ GPa (1.60 Msi)

$G_{12} = 6.20$ GPa (0.9 Msi) $G_{23} = 3.78$ GPa (0.55 Msi)

$\nu_{12} = 0.28$ $\nu_{23} = 0.34$

with a mass density of 1540 kg/m^3 (0.0556 lb/in.^{3}) and a per ply thickness of 0.134 mm (0.00528 in.).

V. Results

Impact experiments were carried out at four velocities on five sizes of specimens, using projectiles of three different diameter tips for each specimen size. In general, the results were quite reproducible among replicate specimens. Some difficulty was experienced with strain gage failure, particularly in the x direction and with the large strain gages. In an attempt to verify that the experiments followed the scaling rules, the strain responses in the y direction measured behind the impact point (location A in Fig. 3) for five sizes of specimens are given in Fig. 4, all at the same impact velocity of 4.57 m/s (15 ft/s). The strain responses in the x direction measured away from the impact center (location B in Fig. 3) for three sizes of specimens $\lambda = 1$, 2, and 4 are given in Fig. 5, also at a velocity of 4.57 m/s. Here the time scale has been multiplied by $1/\lambda$, in accordance with the time scaling discussed above. The results indicate that the strain in the different plate sizes exhibits the same response if time is scaled by λ. Clearly, this is a strong verification of the scaling rules.

Figure 6 shows the strain responses of the 100-mm (4 in.) specimens to the 3.18, 6.35, and 12.7 mm (⅛, ¼, and ½ in.) diameter tup projectiles with mass of 23 gm (0.051 lb), at an impact velocity of 4.57 m/s. The response shows a relatively small effect of the tup diameter. Clearly, the contact stiffness, which varies with the impact tup size as shown in Eq. (20), does not play a major role in the response. This lack of sensitivity to the contact stiffness was also observed in the analysis results.

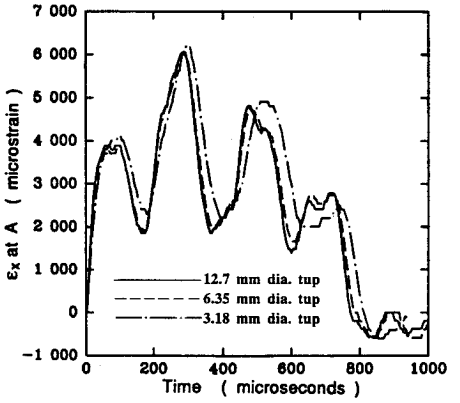

Fig. 6 Measured strain response at location A in 100-mm plate for three different tup sizes, $V_0 = 4.57$ m/s.

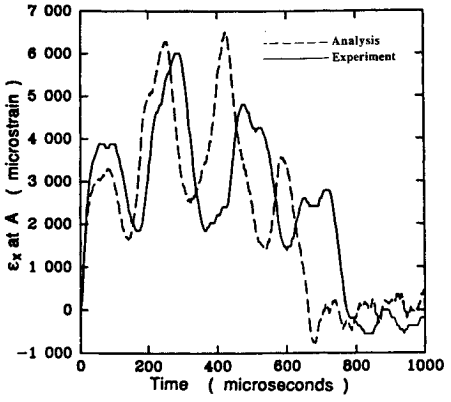

Fig. 7 Comparison of analysis with experiment for ϵ_x at location A in 100-mm plate, $V_0 = 4.57$ m/s.

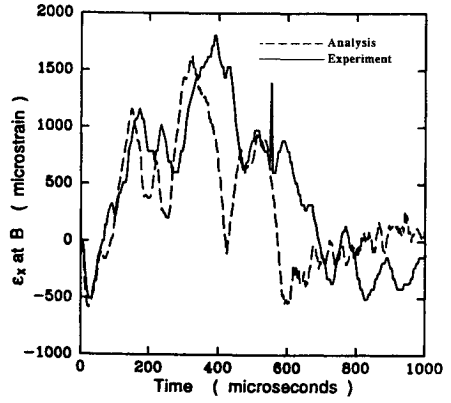

Fig. 8 Comparison of analysis with experiment for ϵ_x at location B in 100-mm plate, $V_0 = 4.57$ m/s.

Figures 7 and 8 show the comparison of the measured and predicted x-direction strain response on the back side of the plate at the impact point and at a distance away from the impact center, corresponding to locations A and B, respectively, in Fig. 3. It can been seen that the strain compares very well between analysis and experiment. The predicted period is somewhat less than the measured value, which was observed in all of the comparisons.

Figures 9 and 10 give the measured peak strain at locations A and B of the specimens, along with the predicted peak values. Basically, the strain varied almost linearly with the impact velocity, indicating that the nonlinear effects associated with the indentation are not particularly significant. The analysis gives a very good prediction for the peak strain away from the impact center. It is noticed that there is a significant difference between predicted and measured peak strains behind the impact point at the higher impact velocities. This probably is due to material damage effects being neglected in the dynamic model.

The experiments were carried out so that damage would be developed in the plates at higher impact velocities. This damage took the form of indentation at the impact point, matrix cracking, broken fibers, and delamination. An extensive program to determine the level of damage in the specimens is underway. Some results will be reported in Ref. 24.

VI. Discussion

Economic considerations of design and testing of large composite structures have led to a growing interest in the use of structural scale model testing and the application of the principles of similitude to the design evaluation of fiber composite components. It is, therefore, very important to understand scaling of experimental results. In the present study, the experimentally measured impact response in the different-sized plates was compared with the scaling rules obtained by examining the linearized impact response problem. The results shown in Figs. 4 and 5 indicate that the strains in the geometrically scaled plates exhibit the same response at constant impact velocity if time is scaled by λ and the impactor mass is scaled by λ^3.

The use of the contact indentation stiffness is important in the analysis, as distributing the contact force over the contact area eliminates the singularity in strain predicted for a point load. On the other hand, both the experiments and the analysis were not particularly sensitive to the specific values used for the contact stiffness. For example, Fig. 6 shows that the experimentally measured strains behind the impact point were not sensitive to the size of the impact tip. Furthermore, the linearity of the strains with impact velocity shown in Figs. 9 and 10 indicates that the nonlinearity associated with the contact stiffness is not a major factor in determining the impact response of the plate. The analytical results also supported this point.

The formation of damage will be subject to scaling laws more complicated than that governing the linear structural response. As discussed by Morton,[20] if the failure processes follow a fracture-mechanics model, size effects will be important and strength will not scale. The trend will be for smaller specimens to be stronger. Work done in the present program[24] supports this view, in which the larger specimens showed significantly more delamination than their smaller counterparts.

The convergence of the Rayleigh-Ritz procedure was also examined. Because of the symmetric geometry of the plate and impact loading, only those mode shapes symmetric about the plate center were involved in the calculation. The numbers of assumed modes used ranged from 8×8 to 20×20. The results showed convergence of strain behind the impact point when the number of modes reached 15×15. This is true for these particular plates under the clamped-clamped and free-free boundary conditions used at present. The analysis results also showed that even higher modes should be included to obtain good accuracy for strains if the boundary conditions were

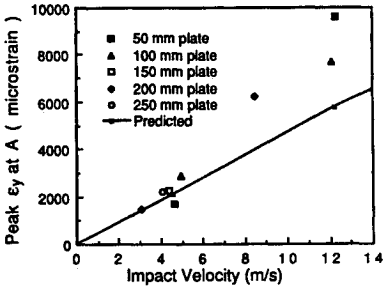

Fig. 9 Effect of impact velocity on ϵ_y at location A for five different plate sizes with largest tups.

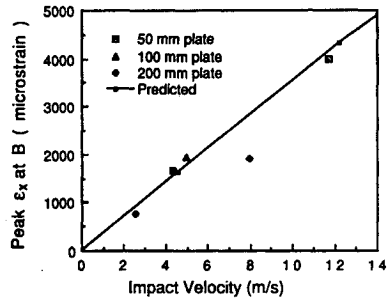

Fig. 10 Effect of impact velocity on ϵ_x at location B for three different plate sizes with largest tups.

changed to simply supported conditions. It is important to choose an appropriate number of assumed modes for a given plate and given boundary conditions.

VII. Summary and Conclusions

The scaling rules for laminated plates subjected to impact loading were obtained from the differential equations governing the linear impact problem. An experimental program was conducted on AS4/3501-6 carbon/epoxy laminates to determine the accuracy of the scaling. This was accomplished by scaling the dimensions of the plates, impactors, and strain gage sizes by a factor ranging from one to five. The measured strain responses at velocities where significant material damage was not produced were found to follow the scaling very closely. An analysis based on the dynamic equations showed excellent agreement with the experiments, and supported the conclusions of the experiments regarding scaling rules.

Acknowledgments

The support of Hercules Aerospace is gratefully acknowledged. Discussions with Ralph Nuismer, Doug Cairns, and Ron Bucinell of Hercules were very helpful.

References

[1]Labor, J. D., "Impact Damage Effects on the Strength of Advanced Composites," *Nondestructive Evaluation and Flaw Criticality for Composite Materials, ASTM STP,* Vol. 696, 1979, pp. 172–184.

[2]Ross, C. A., and Sierakowski, R. L., "Studies on the Impact Resistance of Composite Plates," *Composites,* Vol. 4, 1973, pp. 157–161.

[3]Starnes, J. H., Rhodes, M. D., and Williams, J. G., "Effect of Impact Damage and Holes on the Compressive Strength of a Graphite/Epoxy Laminate," *Nondestructive Evaluation and Flaw Criticality for Composite Materials, ASTM STP,* Vol. 696, 1979, pp. 145–171.

[4]Takeda, N., Sierakowski, R. L., and Malvern, L. E., "Microscopic Observations of Cross Sections of Impacted Composite Laminates," *Composites Technology Review,* Vol. 4, No. 2, 1982, pp. 40–44.

[5]Caprino, G., "Residual Strength Prediction of Impacted CFRP Laminates," *Journal of Composite Materials,* Vol. 18, Nov. 1984, pp. 508–518.

[6]Sun, C. T., and Chattopadhyay, S., "Dynamic Response of Anisotropic Laminate Plates Under Initial Stress to Impact of a Mass," *Journal of Applied Mechanics,* Vol. 42, Sept. 1975, pp. 693–698.

[7]Sun, C. T., and Wang, T., "Dynamic Response of a Graphite/Epoxy Laminated Beam to Impact of Elastic Spheres," NASA-CR-165461, Sept. 1982.

[8]Yang, S. H., and Sun, C. T., "Indentation Law for Composite Laminates," *Composite Materials: Testing and Design (Sixth Conference), ASTM STP,* Vol. 787, 1982, pp. 425–449.

[9]Tan, T. M., and Sun, C. T., "Use of Statical Indentation Laws in the Impact Analysis of Laminated Composite Plates," *Journal of Applied Mechanics,* Vol. 52, March 1985, pp. 6–12.

[10]Takeda, N., Sierakowski, R. L., and Malvern, L. E., "Wave Propagation Experiments on Ballistically Impacted Composite Laminates," *Journal of Composite Materials,* Vol. 15, March 1981, pp. 157–174.

[11]Daniel, I. M., Liber, T., and LaBetz, R. H., "Wave Propagation in Transversely Impacted Composite Laminates," *Experimental Mechanics,* Vol. 19, Jan. 1979, pp. 9–16.

[12]Moon, F. C., "A Critical Survey of Wave Propagation and Impact in Composite Materials," NASA-CR-121226, 1973.

[13]Moon, F. C., "Theoretical Analysis of Impact in Composite Plates," NASA-CR-121110, 1972.

[14]Dobyns, A. L., "Analysis of Simply Supported Orthotropic Plates Subject to Static and Dynamic Loads," *AIAA Journal,* Vol. 19, May 1981, pp. 642–650.

[15]Cairns, D. S., and Lagace, P. A., "Transient Response of Graphite/Epoxy and Kevlar/Epoxy Laminates Subjected to Impact," 29th Structures, Structural Dynamics and Materials Conference Willamsburg, VA (not published in Proceedings), 1988.

[16]Ramkumar, R. L., and Chen, P. C., "Low-Velocity Impact Response of Laminated Plates," *AIAA Journal,* Vol. 21, Oct. 1983, pp. 1448–1452.

[17]Avva, V. S., "Effect of Specimen Size on the Buckling Behavior of Laminated Composites Subjected to Low-Velocity Impact," *Compression Testing of Homogeneous Materials and Composites, ASTM STP,* Vol. 808, 1983, pp. 140–154.

[18]Whitney, J. M., and Pagano, N. J., "Shear Deformation in Heterogeneous Anisotropic Plates," *Journal of Applied Mechanics,* Vol. 37, Dec. 1970, pp. 1031–1036.

[19]Birman, V., and Bert, C. W., "Behavior of Laminated Plates Subjected to Conventional Blast," *International Journal of Impact Engineering,* Vol. 6, 1987, pp. 145–155.

[20]Morton, J., "Scaling of Impact-Loaded Carbon-Fiber Composites," *AIAA Journal,* Vol. 26, No. 8, 1988, pp. 989–994.

[21]Vinson, J. R., and Sierakowski, R. L., *The Behavior of Structures Composed of Composite Materials,* Martinus Nijhoff, Dordrecht, the Netherlands, 1986, Chap. 2.

[22]Vinson, J. R., *Structural Mechanics: The Behavior of Plates and Shells,* Wiley-Interscience, John Wiley and Sons Inc., 1974.

[23]Timoshenko, S., and Young, D. H., *Vibration Problems in Engineering,* 3rd ed., D. Van Nostrand, New York, 1955.

[24]Qian, Y., Swanson, S. R., Nuismer, R. J., and Bucinell, R. B., "An Experimental Study of Scaling Rules for Impact Damage in Fiber Composites," *Journal of Composite Materials,* 1990.